PRP Pharmacology Research & Perspectives
Open Access

ORIGINAL ARTICLE

The putative P-gp inhibitor telmisartan does not affect the transcellular permeability and cellular uptake of the calcium channel antagonist verapamil in the P-glycoprotein expressing cell line MDCK II MDR1

Lasse Saaby[1,2], Peer Tfelt-Hansen[3] & Birger Brodin[2]

[1]Bioneer:FARMA, Faculty of Health and Medical Sciences, University of Copenhagen, Glostrup Hospital, Glostrup, Denmark
[2]Department of Pharmacy, Faculty of Health and Medical Sciences, University of Copenhagen, Copenhagen, Denmark
[3]Danish Headache Center, Department of Neurology, Glostrup Hospital, University of Copenhagen, Glostrup, Denmark

Keywords
Blood–brain barrier, cluster headache, P-glycoprotein, telmisartan, verapamil

Correspondence
Birger Brodin, Department of Pharmacy, Faculty of Health and Medical Sciences, University of Copenhagen, Copenhagen, Denmark. Tel: +45 35336169; Fax: +45 35336001;
E-mail: birger.brodin@sund.ku.dk

Funding Information
Birger Brodin was funded by the Lundbeck Foundation via the project grant "Research Initiative on Brain Barriers and Drug Delivery."

Received: 9 March 2015; Revised: 15 April 2015; Accepted: 18 April 2015

Pharma Res Per, 3(4), 2015, e00151, doi: 10.1002/prp2.151

doi: 10.1002/prp2.151

Abstract

Verapamil is used in high doses for the treatment of cluster headache. Verapamil has been described as a P-glycoprotein (P-gp, ABCB1) substrate. We wished to evaluate in vitro whether co administration of a P-gp inhibitor with verapamil could be a feasible strategy for increasing CNS uptake of verapamil. Fluxes of radiolabelled verapamil across MDCK II MDR1 monolayers were measured in the absence and presence of the putative P-gp inhibitor telmisartan (a clinically approved drug compound). Verapamil displayed a vectorial basolateral-to-apical transepithelial efflux across the MDCK II MDR1 monolayers with a permeability of 5.7×10^{-5} cm sec^{-1} compared to an apical to basolateral permeability of 1.3×10^{-5} cm sec^{-1}. The efflux could be inhibited with the P-gp inhibitor zosuquidar. Zosuquidar (0.4 μmol/L) reduced the efflux ratio ($P_{B\text{-}A}$/$P_{A\text{-}B}$) for verapamil 4.6–1.6. The presence of telmisartan, however, only caused a slight reduction in P-gp-mediated verapamil transport to an efflux ratio of 3.4. Overall, the results of the present in vitro approach indicate, that clinical use of telmisartan as a P-gp inhibitor may not be an effective strategy for increasing brain uptake of verapamil by co-administration with telmisartan.

Abbreviations

A-B, apical-to-basolateral; B-A, basolateral-to-apical; BBB, blood–brain barrier; FBS, fetal bovine serum; HBSS, Hank's balanced salt solution; HEPES, 2-[4-(2-hydroxyethyl)piperazin-1-yl]ethanesulfonic acid; MDCKII, Madin-Darby canine kidney cells type II; PET, positron emission tomography; TEER, transepithelial electrical resistance.

Introduction

The calcium channel inhibitor verapamil is used in the treatment of cluster headache (Evers 2010; Nesbitt and Goadsby 2012; Tfelt-Hansen and Jensen 2012). Cluster headache is characterized by recurrent attacks of severe or excruciating unilateral pain in or around one eye with a duration of 15–180 min and with associated autonomic symptoms (Tfelt-Hansen and Jensen 2012), and is most likely generated in the hypothalamus (Goadsby 2002; Sanchez del Rio and Alvarez Linera 2004; May et al. 2006; Waldman and Goadsby 2006; Tfelt-Hansen and Tfelt-Hansen 2009). It can occur up to eight times a day and is arguably one of the most severe pain syndromes which afflict humans (Tfelt-Hansen and Jensen 2012). Verapamil, given in a daily dose of 360 mg, had some preventive effect on cluster headache (Leone et al. 2000; May et al. 2006; Tfelt-Hansen and Jensen 2012), but in clinical practice, however, daily doses of 480–960 mg, and rarely 1200 mg verapamil, are needed for adequate pain control (May et al. 2006; Cohen et al. 2007; Tfelt-Hansen and Jensen 2012). Doses of this magnitude are considerably

higher than doses normally used in cardiology (Tfelt-Hansen and Tfelt-Hansen 2009) and carries an increased risk of arrhythmias caused by prolongation of the electrical conduction of the heart (Cohen et al. 2007). In a study of 108 cluster headache patients treated with verapamil in doses between 240 and 960 mg/day, 19% had arrhythmia: 12% had first-degree heart block (PR > 200 msec), one had second-degree heart block, and one required a permanent pacemaker (Cohen et al. 2007). The high doses of verapamil needed in cluster headache prevention are most likely due to a general low uptake of verapamil across the blood–brain barrier (BBB) and into the brain. With a log *P*-value of 3.2 (Wienen et al. 2000), verapamil can be considered a relatively lipophilic compound, and is thus expected to easily cross the BBB. However, by means of [^{11}C]-verapamil positron emission tomography (PET) and microdosing in humans, Bauer et al. (2012) found that the brain uptake of verapamil, in the absence of inhibitors to be low and restricted to the choroid plexus and venous sinus. In addition, Römermann et al. (2013) reported that the brain-to-blood ratio of [^{11}C]-verapamil was increased in MDR1- and MDR1/BCRP-knockout mice compared to wild-type and MRP1- and BCRP-knockout mice, indicating that brain uptake of verapamil is restricted by P-glycoprotein (P-gp)-mediated efflux transport. In agreement with these findings, coadministration of tariquidar, a P-gp inhibitor, has been shown to increase brain uptake and distribution of [^{11}C]-verapamil in the brain parenchyma in both humans and rats (Bauer et al. 2012; Müllauer et al. 2012).

The aim of the present study was to investigate in vitro whether a clinically approved drug compound with P-gp inhibitory activity could be used to increase verapamil transport across a P-gp-expressing cell barrier. We chose Madin-Darby canine kidney cells type II (MDCK II) expressing human P-gp as a model cell line, in order to evaluate whether inhibitor coadministration with verapamil might increase transcellular transport of verapamil. The MDCK II cell line is a subclone of the MDCK cell line, originally derived from kidney tissue from a normal cocker spaniel. MDCK cells differentiate into columnar epithelium with functional tight junctions when they are grown as monolayers on polycarbonate permeable filter supports (Cho et al. 1989; Irvine et al. 1999). MDCK II cells transfected with the human ABCB1 (MDR1) gene coding for P-gp have previously been used to identify substrates and inhibitors of P-gp (Guo et al. 2002; Williams et al. 2003; Keogh and Kunta 2006). Tariquidar and other third generation P-gp inhibitors have, however not yet been approved for clinical use. We, therefore, chose telmisartan, a nonpeptide angiotensin-II type 1-receptor antagonist primarily used in the management of hypertension (McClellan and Markham 1998; Deppe et al. 2010), as an inhibitor since this drug previously has been reported to be an inhibitor of P-gp with an IC_{50}-value of 0.38 μmol/L (Weiss et al. 2010).

We observed that verapamil displayed a vectorial basolateral-to-apical (B-A) transepithelial efflux across the MDCK II MDR1 monolayers, and that this net efflux could be inhibited by the P-gp inhibitor zosuquidar. Telmisartan, however, only caused a slight inhibition of P-gp-mediated verapamil transport. This in vitro approach indicates that clinical use of telmisartan as a P-gp inhibitor is not likely to be an effective strategy for increasing brain uptake of verapamil by coadministration with telmisartan.

Materials and Methods

Fetal bovine serum (FBS) was from Gibco, Fischer Scientific (Slangerup, Denmark), penicillin and Strepotmycin from BioWhittaker Cambrex (Vallensbaek, Denmark), Hank's balanced salt solution (HBSS) was from Invitrogen (Taastrup, Denmark), and 2-[4-(2-hydroxyethyl)piperazin-1-yl]ethanesulfonic acid (HEPES) from AppliChem GmbH (Darmstadt, Germany). Plastic ware such as T-75 culture flasks and Transwell® Permeable supports (1.13 cm^2, 0.4 μm pore size) were purchased from Corning, Fischer Scientific.

The radiolabeled isotopes [^{3}H]-digoxin (29.8 Ci/mmol), [^{14}C]-mannitol (0.0571 Ci/mmol), and [^{3}H]-verapamil (0.0815 Ci/mmol) together with Ultima Gold scintillation fluid were purchased from Perkin Elmer Life and Analytical (Boston, MA). Telmisartan was purchased from Sequoia Research Products Ltd. (Pangbourne, UK) Zosuquidar (LY335979, ZSQ) was from Selleck Chemicals (Munich, Germany). All other compounds and reagents were bought from Sigma-Aldrich (Brøndby, Denmark) unless otherwise stated.

Cell culture and maintenance

MDCK-II wild-type and MDR1 cells were kindly provided by Prof. Piet Borst (the Netherlands Cancer Institute, Amsterdam, Netherlands). MDCK II cells were maintained in DMEM (Dulbecco's modified Eagle's medium) supplemented with 10% FBS, penicillin (90 U/mL), streptomycin (90 μg/mL), and 10% of both L-glutamine and nonessential amino acids. The cells were cultured in T-75 culture flasks (5% CO_2, 37°C) and subcultured when reaching approximately 80–90% confluence. For transport studies, cells were seeded onto permeable 12 mm polycarbonate filter supports (Transwell, Corning) at a density of 1.6×10^5 cells/filter. Culture medium was changed every other day in both the apical and basolateral chamber.

Transepithelial transport experiments

Bidirectional transepithelial transport of 0.03 μmol/L [^{3}H]-digoxin, 17.5 μmol/L [^{14}C]-mannitol, and 12 μmol/L [^{3}H]-verapamil was measured across MDCK II (MDR1) cells after 1–2 days of culture on filter supports. Transport buffer was HBSS supplemented with 10 mmol/L HEPES (pH 7.4), 0.05% BSA, and 0.04% sodium bicarbonate. Transepithelial electrical resistance (TEER) was measured prior to each transport experiment using an Endohm 12 cup electrode chamber (World Precision Instruments Inc., Sarasota, FL) connected to a voltohmmeter (EVOM; World Precision Instruments Inc.) at room temperature. The resistance of empty filter supports was between 11 and 12 Ωcm^2, while the mean resistance across MDCK II (MDR1) was 271 $\pm$ 129 Ωcm^2 (n = 236). Prior to transport experiments, the cells were preincubated in transport buffer for 30 min. Transport experiments were initiated by replacing the existing transport buffer with transport buffer containing either [^{3}H]-digoxin or [^{3}H]-verapamil, both in combination with [^{14}C]-mannitol, on either the apical or the basolateral side. All radioactive compounds were used at a concentration of 1 μCi/mL. For experiments involving telmisartan, a stock solution of 0.48 mmol/L telmisartan in dimethyl sulfoxide (DMSO) was added to the transport buffer (in both apical and basolateral compartments) to give a final concentration of 2.4 μmol/L and a DMSO concentration of 0.5%. 0.5% DMSO was also added the transport buffer in control treatments. For experiments containing zosuquidar, a stock solution of 5 mmol/L in purified water, was added to the transport buffer (in both apical and basolateral compartments) to give a final concentration of 0.4 μmol/L. Transport experiments were performed at 37°C under circular rotation (95 rpm) on a KS15 Edmund Bühler Compact Shaker (Holm and Halby, Broendby, Denmark). About 100 μL samples were taken from the basolateral compartment at t = 15, 30, 45, 60, 90, and 120 min in the apical-to-basolateral (A-B) transport experiments. For B-A transport, 50 μL samples were taken from the apical compartment (0.5 mL) at the same time points. The withdrawn sample volumes were replaced with blank transport buffer. The withdrawn samples were transferred to scintillation vials and 2 mL scintillation fluid was added. The radioactivity of the samples was determined in a liquid scintillation analyzer (Packard Tri-Carb 2100 TR; Canberra, Dreich, Germany).

Data analysis

TEER values were standardized by multiplying with the cross-sectional area of the filter supports.

The apparent permeability coefficients (Papp) of transepithelial transport of [^{3}H]-digoxin, [^{14}C]-mannitol, and [^{3}H]-verapamil verapamil were calculated using equation (1):

$$P_{app} = \frac{J}{C_0} = \frac{Q_t}{C_0 A t} \quad (1)$$

where J is the steady-state flux (nmol cm-2 min-1), C_0 is the initial concentration in the donor compartment, A is the area of the filter support (1.13 cm^2), and Q_t is the accumulated amount of compound (nmol) in the receiver compartment at time t (minutes). The flux of the transported compound was calculated as the slope of the straight part of the line from a plot of Q_t versus time, thus correcting for lag time effects.

Donor samples were taken at the beginning and at the end of each experiment to ensure that steady-state conditions (less than 10% of the total amount of compound transported) were present throughout the experiment. Efflux ratios were calculated by dividing the apparent permeability coefficient for basolateral to apical transport with the apparent permeability coefficient for apical to basolateral transport.

Permeability coefficients and efflux ratios were compared using a paired or unpaired Student's t-test to test for significant difference between populations (α = 0.05).

Results

In the present study, we investigated in vitro whether inhibition of P-gp might cause an increase in transepithelial A-B verapamil transport across a model cell line expressing P-gp in the apical membrane. Bidirectional transport experiments were performed on MDCK II-MDR1 cells, grown in monolayers for 1 day. Transport of verapamil and digoxin was investigated, in the absence and presence of the well-characterized P-gp inhibitor zosuquidar and the compound telmisartan which has been described as a P-gp inhibitor.

[^{3}H]-labeled verapamil displayed a net efflux in the B-A direction in MDCK-II (MDR1) cell monolayers

The transepithelial transport of [^{3}H]-verapamil across MDCK II (MDR1) cell monolayers was measured in both the A-B and the B-A direction. The flux of [^{3}H]-verapamil was higher in the B-A direction than the flux in the A-B direction, indicating a vectorial net transport of the compound in the B-A direction (Fig. 1). The flux of [^{3}H]-verapamil was not constant over the entire time course of the experiments. This was especially pronounced for the B-A fluxes (Fig. 1). The observed

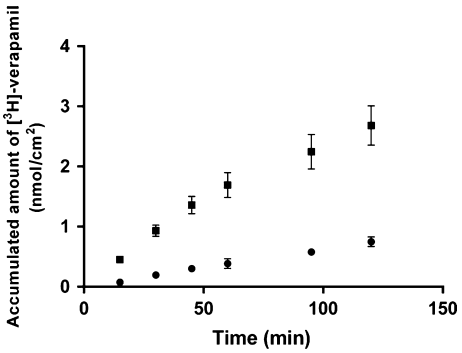

Figure 1. Transepithelial transport of [^{3}H]-verapamil (12 μmol/L) across MDCK II (MDR1) in the apical to basolateral (closed circles) and the basolateral to apical direction (closed squares). Data show accumulation of verapamil on the acceptor side as a function of time. Data points represent the means, while error bars designate the standard deviations (n = 9, N = 3).

time-dependent change in fluxes was probably caused by a change in the concentration gradient of [^{3}H]-verapamil across the MDCK II (MDR1) cells, which, in turn, is caused by a high initial transport rate. Fluxes, for calculation of permeabilities, were therefore extrapolated from the linear part of the accumulation curves, as described in methods. The A-B permeability of [^{3}H]-verapamil was estimated to be $1.3 \pm 0.2 \times 10^{-5}$ cm sec^{-1} (n = 15, N = 3) which was significantly lower ($P < 0.0001$) than the permeability in the B-A direction of $5.5 \pm 0.8 \times 10^{-5}$ cm sec^{-1} (n = 15, N = 3). The efflux ratio $P_{B\text{-}A}/P_{A\text{-}B}$ was 4.4. In comparison, the efflux ratio of the paracellular flux marker [^{14}C]-mannitol was ~1.5. Ideally this efflux ratio will be 1 if no net transport occurs, however, in practice the B-A flux of mannitol may be slightly larger than the A-B flux in the presence of agonists and their solvents, probably due to a slight interference with tight junctions. The small increase in paracellular permeability is not likely to influence the larger transcellular efflux of verapamil.

The bidirectional transport of verapamil across MDCK II (MDR1) cells was measured in the presence and in the absence of the known P-gp inhibitor zosuquidar (Slate et al. 1995; Dantzig et al. 1996) in order to investigate whether the observed B-A efflux of [^{3}H]-verapamil was mediated by P-gp, (Fig. 2A). In the presence of 0.4 μmol/L zosuquidar the B-A permeability of [^{3}H]-verapamil was $3.8 \pm 0.4 \times 10^{-5}$ cm sec^{-1} (n = 9, N = 3) which was significantly lower ($P < 0.0001$) than the observed B-A permeability of $5.7 \pm 0.8 \times 10^{-5}$ cm sec^{-1} (n = 9, N = 3) in the absence of zosuquidar. Correspondingly, the A-B transport of [^{3}H]-verapamil increased significantly ($P < 0.0001$) from $1.3 \pm 0.2 \times 10^{-5}$ cm sec^{-1} (n = 9, N = 3) in the absence of zosuquidar, to $2.3 \pm 0.2 \times 10^{-5}$ cm sec^{-1} (n = 9, N = 3) in the presence of 0.4 μmol/L zosuquidar (Fig. 2A). Correspondingly, the efflux ratio of verapamil was significantly reduced ($P < 0.0001$) from 4.3 ± 0.4 (n = 3, N = 3) in the absence of zosuquidar to 1.6 ± 0.2 (n = 3, N = 3) in the presence of 0.4 μmol/L zosuquidar (Fig. 2B). Overall, the presence of 0.4 μmol/L zosuquidar reduced the efflux ratio $P_{B\text{-}A}/P_{A\text{-}B}$ of verapamil to a magnitude similar to that of the paracellular flux-marker mannitol, indicating that verapamil was a substrate for, and that the observed vectorial efflux of verapamil was caused solely by P-gp in the MDCK II (MDR1) cell monolayers.

Transcellular permeability and cellular uptake of verapamil was only slightly affected by the presence of telmisartan in MDCK II (MDR1) cell monolayers

The bidirectional transepithelial transport of [^{3}H]-verapamil was measured in the presence and absence of telmisartan in order to investigate whether telmisartan affects the transport of verapamil across MDCK II (MDR1) cells (n = 6, N = 3). A relatively high concentration of 2.4 μmol/L telmisartan was chosen, as pilot experiments showed no effects at low concentrations (data not shown). The presence of telmisartan caused a small and not statistically significant decrease in B-A permeability, from $5.3 \pm 0.9 \times 10^{-5}$ cm sec^{-1} (n = 6, N = 3) in the absence of telmisartan to $4.9 \pm 0.5 \times 10^{-5}$ cm sec^{-1} (n = 6, N = 3) in the presence of 2.4 μmol/L telmisartan. Correspondingly, the A-B permeability increased from $1.3 \pm 0.2 \times 10^{-5}$ cm sec^{-1} (n = 6, N = 3) in the absence of telmisartan to $1.5 \pm 0.3 \times 10^{-5}$ cm sec^{-1} (n = 6, N = 3) in the presence of telmisartan. A pairwise comparison of the mean A-B permeabilities of verapamil with the corresponding permeabilities in the presence of telmisartan within each cell passage (Fig. 3A), showed that the A-B permeability of verapamil was marginally increased in the presence of 2.4 μmol/L of telmisartan in five out of six passages. In a paired t-test, the observed increase in A-B permeability was statistically significant at a confidence level of 0.05 (P = 0.0465). Similarly, by plotting the efflux ratios of [^{3}H]-verapamil in the presence and absence of 2.4 μmol/L telmisartan shows that the efflux ratio was lower in the presence of telmisartan in five out of six passages (Fig. 3B). However, the observed decrease in [^{3}H]-verapamil efflux ratio was not statistically significant at a confidence level of 0.05. The effects of telmisartan on verapamil efflux thus indicate that telmisartan may cause a minor inhibition of the transepithelial efflux of [^{3}H]-verapamil in MDCK II (MDR1) cell monolayers. The amount of [^{3}H]-verapamil present in cells after a transepithelial transport in the A-B direction was measured in order to evaluate the influence of telmisartan

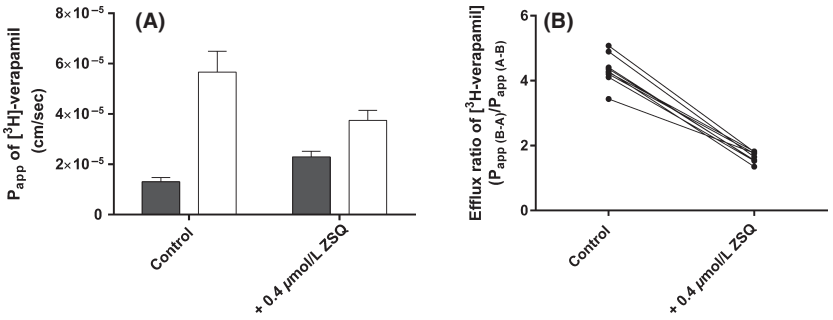

Figure 2. (A) The apparent transepithelial permeability of [3H]-verapamil (12 μmol/L) in the apical to basolateral (grey bars) and basolateral to apical (white bars) direction across MDCK II (MDR1) cells in the presence or absence of zosuquidar (ZSQ, 0.4 μmol/L). Data represent the means $\pm$ SD (n = 9, N = 3). (B) Efflux ratios for [3H]-verapamil (12 μmol/L) across MDCK II (MDR1) cells in the presence or absence of zosuquidar (ZSQ, 0.4 μmol/L). Data points represent the calculated efflux ratio for individual cell culture passages (n = 9). Efflux ratio was calculated as the ratio between the basolateral to apical and the apical to basolateral apparent permeability from means of three filters (N = 3) for each treatment and direction. Connected data points originate from the same cell culture passage.

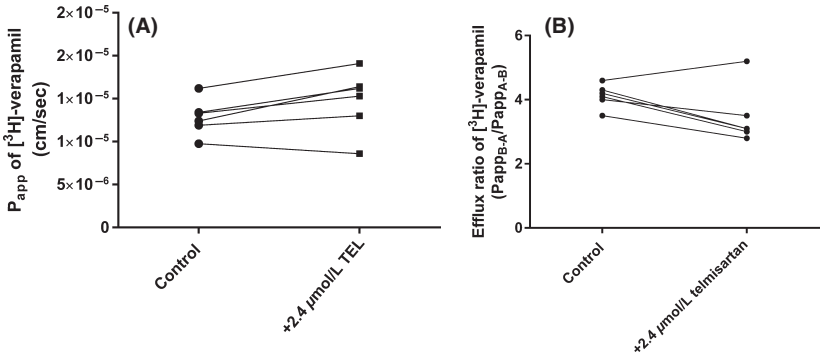

Figure 3. (A) The apparent transepithelial permeability of ^{3}H-verapamil (12 μmol/L) in the apical to basolateral direction across MDCK II (MDR1) cells in the presence or absence of telmisartan (TEL, 2.4 μmol/L). Data points represent the mean permeability of three filter supports (N = 3) of six different passages (n = 6). Lines between data points indicate how the data points are paired within each of the six cell passages. The effect of zosuquidar on the A-B transport of verapamil was statistically significant in a paired t-test (P = 0.0465). (B) Efflux ratio for ^{3}H-verapamil (12 μmol/L) across MDCK II (MDR1) cells in the presence or absence of telmisartan (TEL, 2.4 μmol/L). Data points represent the calculated efflux ratios for six individual passages (n = 6). Lines between data points indicate how the data points are paired within each of the six cell passages.

and zosuquidar on cellular uptake of [^{3}H]-verapamil (Fig. 4). In the presence of 2.4 μmol/L telmisartan, the amount of [^{3}H]-verapamil present in cells and filter supports was increased to 0.24 $\pm$ 0.02 nmol cm^{-2} (n = 3, N = 3) from 0.19 $\pm$ 0.02 nmol cm^{-2} in the absence of telmisartan ($P < 0.0001$) (n = 6, N = 3). In the presence of 0.4 μmol/L zosuquidar, the amount of [^{3}H]-verapamil present in cells and filter supports was increased to 0.32 $\pm$ 0.02 nmol cm^{-2} ($P < 0.0001$) (n = 3, N = 3). In other words, both telmisartan and zosuquidar, at concentrations of 2.4 and 0.4 μmol/L, respectively, increased the uptake of [^{3}H]-verapamil into MDCK II (MDR1) cells, consistent with a role as P-gp inhibitors. The concentration of verapamil in the presence of telmisartan increased by ~26% as compared to the untreated control, whereas the concentration of verapamil in the presence of zosuquidar increased by ~68%.

Overall, our studies suggested that telmisartan did affect the verapamil transport from cell interior to the apical compartment slightly, but that this only affected the transepithelial B-A net flux of verapamil across MDCK II (MDR1) cell monolayers slightly.

Transcellular permeability and uptake of digoxin was not affected by telmisartan

In order to investigate if a possible inhibitory effect of telmisartan would be more readily detectable when using a P-gp substrate with a higher $P_{B\text{-}A}/P_{A\text{-}B}$ than verapamil, the bidirectional transport of the well-known P-gp substrate [^{3}H]-digoxin across MDCK II (MDR1) cells and the cellular accumulation was measured (Fig. 5A). The flux of [^{3}H]-digoxin was constant over the entire time course of the experiments in both the A-B and the B-A

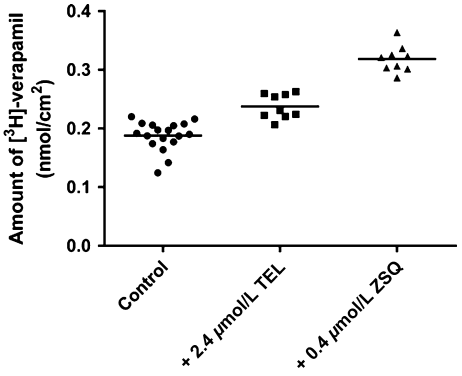

Figure 4. Amount of ^{3}H-verapamil remaining on filter supports including MDCK II (MDR1) cells after an apical to basolateral transport experiment in the presence or absence of telmisartan (TEL, 2.4 μmol/L) or zosuquidar (ZSQ, 0.4 μmol/L). Data were collected from three to six different passages with three filter supports for each treatment and passage (n = 3–6, N = 3). Bars in the scatter plot designate the mean amount of ^{3}H-verapamil found for each treatment. The effect of both telmisartan and zosuquidar on the uptake of verapamil was statistically significant in an unpaired t-test ($P < 0.0001$).

direction with an estimated A-B permeability of $1.4 \pm 0.2 \times 10^{-6}$ cm sec^{-1} (n = 3, N = 3), while the permeability was estimated to be $1.5 \pm 0.1 \times 10^{-5}$ cm sec^{-1} (n = 3, N = 3) in the B-A direction (Fig. 5B). The corresponding efflux ratio was 10.7 in favor of the B-A direction, which indicated a net efflux of [^{3}H]-digoxin across the MDCK II (MDR1) cell monolayers. In the presence of 2.4 μmol/L telmisartan, the A-B and the B-A permeability of [^{3}H]-digoxin was estimated to be $1.5 \pm 0.3 \times 10^{-6}$ cm sec^{-1} and $1.7 \pm 0.1 \times 10^{-5}$ cm sec^{-1} (n = 3, N = 3), respectively (Fig. 5B). The resulting efflux ratio of [^{3}H]-digoxin was 11.2 favor of the B-A direction, which indicates an active efflux of [^{3}H]-digoxin in the presence of 2.4 μmol/L telmisartan. In the same experiments, the efflux ratio of the paracellular flux marker [^{14}C]-mannitol was 1.1.

The amount of [^{3}H]-digoxin present in cells and filter after a transepithelial transport study in the A-B direction in the absence or presence of 2.4 μmol/L telmarisartan was measured in order to evaluate whether telmisartan affects the cellular uptake of [^{3}H]-digoxin. As shown in Figure 6, there were no difference in the amount of [^{3}H]-digoxin present in cells and filter between MDCKII (MDR1) cells incubated in the presence or absence of 2.4 μmol/L telmisartan.

Overall, there were no differences in the estimated permeabilities of [^{3}H]-digoxin and in the corresponding efflux ratios, nor in the amount of [^{3}H]-digoxin in the presence or absence of 2.4 μmol/L telmisartan. These findings indicate, that telmisartan does not affect the transepithelial transport of [^{3}H]-digoxin across MDCK II (MDR1) cells at a concentration of 2.4 μmol/L.

Discussion

Verapamil is a substrate for P-pg in MDCK II (MDR1) cells

PET studies using [^{11}C]-verapamil as a binding ligand have provided evidence showing, that verapamil is a P-gp substrate, however, only few in vitro data are available from cell-based monolayer models. In the present study, the transepithelial transport of [^{3}H]-verapamil was found to be polarized in the B-A direction across MDCK II (MDR1) cells, with efflux ratios ranging between 3.5 and 5.1. In the presence of 0.4 μmol/L of the known P-gp inhibitor zosuquidar, the efflux ratio for [^{3}H]-verapamil was reduced to values of 1.4–1.8 indicating that the observed efflux transport of [^{3}H]-verapamil was primarily mediated by P-gp. These findings are in accordance with previous findings from a bidirectional transport study of verapamil permeability across LLC-PK1 cells (Pauli-Magnus et al. 2000). In this study, the A-B permeability of verapamil was found to be approximately fourfold greater than the corresponding B-A permeability across LLC-PK1 cells stably transfected with MDR1. In contrast, no polarized transport of verapamil was observed across wild-type LLC-PK1 cells, and based on these findings; the authors concluded that the polarized transport of verapamil observed in the MDR1-transfected cells where attributable to the expression of P-gp (Pauli-Magnus et al. 2000). The findings of the present study are further supported by a study by Spoelstra et al. (1994) who investigated the accumulation of verapamil in two human wild-type cancer cell lines (A2780 and SW-1573) and their P-gp-expressing sublines (2780AD and SW1573/1R500) in a flow-through tissue culture system. With this setup it was observed that accumulation of [^{3}H]-verapamil was significantly higher in the wild-type cell lines as compared to the accumulation in the respective P-gp-expressing cell lines, which indicates that verapamil is a substrate for P-gp.

Transcellular permeability and cellular uptake of verapamil is only slightly affected by the presence of telmisartan

Investigating the bidirectional permeability of verapamil in the presence and absence of 2.4 μmol/L telmisartan, we found that the apparent permeability in the A-B direction was reduced and the cellular uptake increased in cells treated with telmisartan. Even though these effects were modest, they indicate that telmisartan is able to modulate the efflux of verapamil across MDCK II (MDR1) cells. However, a corresponding increase in the B-A apparent permeability of verapamil could not be observed.

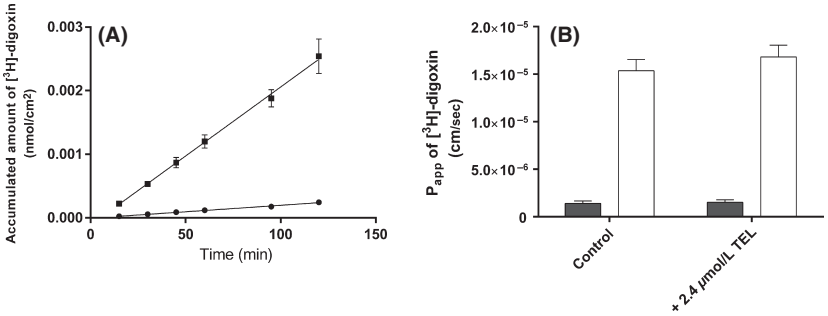

Figure 5. (A) Transepithelial transport of [^{3}H]-digoxin (0.03 μmol/L) across MDCK II (MDR1) cells as a function of time, in the apical to basolateral (closed circles) and the basolateral to apical direction (closed squares). Data show accumulation of digoxin on the acceptor side as a function of time. Data points represent the means, while error bars designate the standard deviations (n = 3, N = 3). (B) The apparent transepithelial permeability of [^{3}H]-digoxin (0.03 μmol/L) in the apical to basolateral (grey bars) and basolateral to apical (white bars) direction across MDCK II (MDR1) cells in the presence or absence of telmisartan (TEL, 2.4 μmol/L). Data represent the means ± SD (n = 3, N = 3).

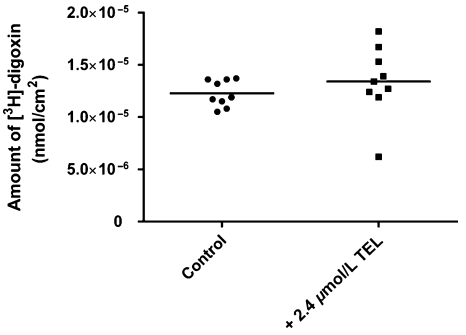

Figure 6. Amount of ^{3}H-digoxin remaining on filter supports including MDCK II (MDR1) cells after an apical to basolateral transport experiment in the presence or absence of telmisartan (2.4 μmol/L). Data were collected from three different passages with three filter support for each treatment and passage (n = 3, N = 3). Bars in the scatter plot designate the mean amount of ^{3}H-digoxin found for each treatment.

Similarly, there was no significant change in the mean efflux ratio of verapamil. To exclude the possibility of the interference from inter-passage variation, we performed a pairwise comparison of the apparent permeabilities of verapamil in the presence or absence of telmisartan within each of the cell passages used. The observed differences were not significant in a paired t-test at a confidence level of 0.05.

Having shown that verapamil is a substrate for P-gp in the MDCK II (MDR1) cells, we turned to investigate whether telmisartan affects the P-gp activity by measuring the bidirectional transport of [^{3}H]-digoxin in the presence and absence of 2.4 μmol/L telmisartan. Digoxin is a known substrate for P-gp and is a widely used marker for P-gp efflux activity (Ma et al. 2010). As expected, an active efflux of digoxin was observed across the MDCK II (MDR1) cells, which remained unchanged in the presence of telmisartan. Correspondingly, no difference in the cellular uptake of digoxin could be observed between transport experiments in the absence and presence of telmisartan. These observations indicate that the P-gp functionality of the MDCK II (MDR1 cells was unaffected by telmisartan. These observations are, however, in contrast to a previous study by Kamiyama et al. (2010) where telmisartan and other angiotensin II type 1 receptor blockers were shown to inhibit the efflux transport of digoxin across Caco-2 cells. In this study, the effect of telmisartan on digoxin efflux was investigated at concentrations between 0.03 and 30 μmol/L, and from these experiments the authors estimated an IC50-value of 2.2 μmol/L. The majority of the proposed effect of telmisartan on the P-gp function in Caco-2 cells was observed over a relatively narrow concentration range of 1–3 μmol/L. Aqueous solubility of telmisartan has been reported to be in the range of 0.45 μmol/L (Park et al. 2013) to as low as 0.17 μmol/L (Tran et al. 2008). The transport study by Kamiyama et al. (2010) was conducted in HBSS (pH 7.4) with no addition of solvents (e.g., DMSO) and it is therefore not unlikely, that telmisartan may have precipitated out of solution in samples with concentrations above 0.5 μmol/L. In MDCK II cells transfected with the human MDR1 gene Chang et al. (2006) found that telmisartan at a concentration of 5 μmol/L was able to inhibit the efflux transport of digoxin. However, in the reported transport experiments, the cells were preincubated with telmisartan for 30 min prior to starting the experiments, at which the transport buffer was changed with fresh transport buffer containing an additional amount of telmisartan. As telmisartan is a lipophilic compound with a reported log P of 3.2 (Wienen et al. 2000), it is likely that a considerable amount will accumulate in the plasma membranes of the MDCK II MDR1 cells during the preincubation step. The total exposure to telmisartan in these experiments may be considerably higher than the exposure resulting only from the reported 5 μmol/L telmisartan. The experimental

conditions for the investigations reported by Chang et al. (2006) differ therefore somewhat from the conditions of the present study.

Using the calcein AM uptake assay the P-gp inhibitory effect of telmisartan was investigated in two P-gp overexpressing cell lines and their parent non-P-gp expressing cell lines. Through these investigations, the authors observed that telmisartan inhibited the P-gp activity of the murine cell line P388/dx, but not that of the LMDR1 cells, a porcine kidney epithelial cell line overexpressing human P-gp, as no difference in calcein AM uptake could be observed between the transfected and the parent cell line (Weiss et al. 2010). The authors argued, that the observed differences between the two cell lines could possibly be explained by species differences and a potential telmisartan-mediated inhibition of MRP in the L-MDR1 cells and the parent cell line.

The contradicting findings on the action of telmisartan on verapamil transport reported in this study and in previous studies and between different cell lines could indicate the involvement of other transport systems than P-gp such as another ABC-type transporters or a less well-characterized transporter. An organic cation transporter, which recognizes verapamil as a substrate, has previously been described in human retinal pigment epithelial (Han et al. 2001) and alveolar epithelial cells (Salomon et al. 2014), and in rat retinal capillary endothelial cells (Kubo et al. 2013). The transport properties have been reported to be different from that of known organic cation transporters and to this date the molecular nature if this novel transporter is still unknown. Since verapamil is a substrate for this transporter, its presence in the MDCK II cells could lead to an underestimation of the P-gp-mediated efflux of verapamil.

Conclusions

In the present study, we investigated in vitro whether telmisartan was able to inhibit P-gp activity and thereby increase uptake of verapamil in a P-gp-expressing cell monolayer, the MDCK II (MDR1) cell line. This was not the case, as only a minor inhibition of verapamil efflux and no inhibition of digoxin efflux was observed. Judged from the mechanistic studies presented here, coadministration of telmisartan and verapamil with the aim of increasing brain uptake of verapamil, are not likely to be relevant in a therapeutic context. Our study and previous studies indicate that the observed action of telmisartan on efflux phenomena in previous studies may be influenced by the presence of other transporter systems. The MDCK II cells used in this study do not, as such, model the human BBB, and the findings of the present study only reflect the in vitro interaction between verapamil and telmisartan at P-gp. The role of telmisartan in the context of brain uptake of verapamil should thus be investigated in appropriate animal models before definitive conclusions can be drawn.

Acknowledgements

The authors thank Mette Frandsen, Thara Hussain, and Maria Diana Læssøe Pedersen for expert technical assistance, and Professor Piet Borst from Netherlands Cancer Institute for providing MDR1-MDCK cells. Birger Brodin was funded by the Lundbeck Foundation via the project grant "Research Initiative on Brain Barriers and Drug Delivery."

Disclosures

None declared.

References

Bauer M, Zeitlinger M, Karch R, Matzneller P, Stanek J, Jager W, et al. (2012). Pgp-mediated interaction between (R)-[11C]verapamil and tariquidar at the human blood-brain barrier: a comparison with rat data. Clin Pharmacol Ther 91: 227–233.

Chang C, Bahadduri PM, Polli JE, Swaan PW, Ekins S (2006). Rapid identification of P-glycoprotein substrates and inhibitors. Drug Metab Dispos 34: 1976–1984.

Cho MJ, Thompson DP, Cramer CT, Vidmar TJ, Scieszka JF (1989). The Madin Darby canine kidney (MDCK) epithelial cell monolayer as a model cellular transport barrier. Pharm Res 6: 71–77.

Cohen AS, Matharu MS, Goadsby PJ (2007). Electrocardiographic abnormalities in patients with cluster headache on verapamil therapy. Neurology 69: 668–675.

Dantzig AH, Shepard RL, Cao J, Law KL, Ehlhardt WJ, Baughman TM, et al. (1996). Reversal of P-glycoprotein-mediated multidrug resistance by a potent cyclopropyldibenzosuberane modulator, LY335979. Cancer Res 56: 4171–4179.

Deppe S, Boger RH, Weiss J, Benndorf RA (2010). Telmisartan: a review of its pharmacodynamic and pharmacokinetic properties. Expert Opin Drug Metab Toxicol 6: 863–871.

Evers S (2010). Pharmacotherapy of cluster headache. Expert Opin Pharmacother 11: 2121–2127.

Goadsby PJ (2002). Pathophysiology of cluster headache: a trigeminal autonomic cephalgia. Lancet Neurol 1: 251–257.

Guo A, Marinaro W, Hu P, Sinko PJ (2002). Delineating the contribution of secretory transporters in the efflux of etoposide using Madin-Darby canine kidney (MDCK) cells

overexpressing P-glycoprotein (Pgp), multidrug resistance-associated protein (MRP1), and canalicular multispecific organic anion transporter (cMOAT). Drug Metab Dispos 30: 457–463.

Han YH, Sweet DH, Hu DN, Pritchard JB (2001). Characterization of a novel cationic drug transporter in human retinal pigment epithelial cells. J Pharmacol Exp Ther 296: 450–457.

Irvine JD, Takahashi L, Lockhart K, Cheong J, Tolan JW, Selick HE, et al. (1999). MDCK (Madin-Darby canine kidney) cells: a tool for membrane permeability screening. J Pharm Sci 88: 28–33.

Kamiyama E, Nakai D, Mikkaichi T, Okudaira N, Okazaki O (2010). Interaction of angiotensin II type 1 receptor blockers with P-gp substrates in Caco-2 cells and hMDR1-expressing membranes. Life Sci 86: 52–58.

Keogh JP, Kunta JR (2006). Development, validation and utility of an in vitro technique for assessment of potential clinical drug-drug interactions involving P-glycoprotein. Eur J Pharm Sci 27: 543–554.

Kubo Y, Kusagawa Y, Tachikawa M, Akanuma S, Hosoya K (2013). Involvement of a novel organic cation transporter in verapamil transport across the inner blood-retinal barrier. Pharm Res 30: 847–856.

Leone M, D'Amico D, Frediani F, Moschiano F, Grazzi L, Attanasio A, et al. (2000). Verapamil in the prophylaxis of episodic cluster headache: a double-blind study versus placebo. Neurology 54: 1382–1385.

Ma JD, Tsunoda SM, Bertino JS Jr, Trivedi M, Beale KK, Nafziger AN (2010). Evaluation of in vivo P-glycoprotein phenotyping probes: a need for validation. Clin Pharmacokinet 49: 223–237.

May A, Leone M, Afra J, Linde M, Sandor PS, Evers S, et al. (2006). EFNS guidelines on the treatment of cluster headache and other trigeminal-autonomic cephalalgias. Eur J Neurol 13: 1066–1077.

McClellan KJ, Markham A. (1998) Telmisartan. Drugs 56: 1039–1044, discussion 1045–1036.

Müllauer J, Kuntner C, Bauer M, Bankstahl JP, Muller M, Voskuyl RA, et al. (2012). Pharmacokinetic modeling of P-glycoprotein function at the rat and human blood-brain barriers studied with (R)-[11C]verapamil positron emission tomography. EJNMMI Res 2: 58.

Nesbitt AD, Goadsby PJ (2012). Cluster headache. BMJ 344: e2407.

Park J, Cho W, Cha KH, Ahn J, Han K, Hwang SJ (2013). Solubilization of the poorly water soluble drug, telmisartan, using supercritical anti-solvent (SAS) process. Int J Pharm 441: 50–55.

Pauli-Magnus C, von Richter O, Burk O, Ziegler A, Mettang T, Eichelbaum M, et al. (2000). Characterization of the major metabolites of verapamil as substrates and inhibitors of P-glycoprotein. J Pharmacol Exp Ther 293: 376–382.

Römermann K, Wanek T, Bankstahl M, Bankstahl JP, Fedrowitz M, Muller M, et al. (2013). (R)-[(11)C]verapamil is selectively transported by murine and human P-glycoprotein at the blood-brain barrier, and not by MRP1 and BCRP. Nucl Med Biol 40: 873–878.

Salomon JJ, Ehrhardt C, Hosoya K (2014). The verapamil transporter expressed in human alveolar epithelial cells (A549) does not interact with beta2-receptor agonists. Drug Metab Pharmacokinet 29: 101–104.

Sanchez del Rio M, Alvarez Linera J (2004). Functional neuroimaging of headaches. Lancet Neurol 3: 645–651.

Slate DL, Bruno NA, Casey SM, Zutshi N, Garvin LJ, Wu H, et al. (1995). RS-33295-198: a novel, potent modulator of P-glycoprotein-mediated multidrug resistance. Anticancer Res 15: 811–814.

Spoelstra EC, Westerhoff HV, Pinedo HM, Dekker H, Lankelma J (1994). The multidrug-resistance-reverser verapamil interferes with cellular P-glycoprotein-mediated pumping of daunorubicin as a non-competing substrate. Eur J Biochem 221: 363–373.

Tfelt-Hansen PC, Jensen RH (2012). Management of cluster headache. CNS Drugs 26: 571–580.

Tfelt-Hansen P, Tfelt-Hansen J (2009). Verapamil for cluster headache. Clinical pharmacology and possible mode of action. Headache 49: 117–125.

Tran PH, Tran HT, Lee BJ (2008). Modulation of microenvironmental pH and crystallinity of ionizable telmisartan using alkalizers in solid dispersions for controlled release. J Control Release 129: 59–65.

Waldman A, Goadsby PJ (2006). Synthesis of cluster headache pathophysiology. In J. Olsen, P. J. Goadsby, N. M. Ramadan and P. Tfelt-Hansen, eds. The headaches. Philadelphia, Lippincott Williams & Wilkins, 783–787

Weiss J, Sauer A, Divac N, Herzog M, Schwedhelm E, Boger RH, et al. (2010). Interaction of angiotensin receptor type 1 blockers with ATP-binding cassette transporters. Biopharm Drug Dispos 31: 150–161.

Wienen W, Entzeroth M, van Meel JCA, Stangier J, Busch U, Ebner T, et al. (2000). A review on Telmisartan: a novel, long-acting angiotensin II-receptor antagonist. Cardiovasc Drug Rev 18: 127–154.

Williams GC, Knipp GT, Sinko PJ (2003). The effect of cell culture conditions on saquinavir transport through, and interactions with, MDCKII cells overexpressing hMDR1. J Pharm Sci 92: 1957–1967.